Extended Abstracts of the 2009 International Conference on Solid State Devices and Materials, Sendai, 2009, pp362-363

# Raman Spectroscopic Metrology for Stress measurement in Semiconductor Device Development and Process

Nobuyuki Naka[1], Shinsuke Kashiwagi[1], Kunio Ohtsuki[1], JaeHyun Kim[2], ChangHwan Lee[2], SangTae Ahn[2], KoonHo Bae[2], HyungWon Yoo[2], ChulHong Kim[2]

[1]Semiconductor Systems R&D Department, HORIBA, Ltd., 2 Miyanohigashi, Kisshoin, Minami-ku, Kyoto 601-8510, Japan
Phone: +81-75-313-8121, Fax: +81-75-315-9525, E-mail: nobuyuki.naka@horiba.com
[2]Hynix Semiconductor Inc., San 136-1, Ami-ri Bubal-eub, Icheon-si, Gyeonggi-do, 467-701, Korea

## 1. Introduction

In the semiconductor field, device makers progress to smaller design rules for the logic device as well as memory devices to keep up with Moore's law. With shrinking the pattern size, stress or strain control in the local area will gain great significance for reducing the fluctuation of electrical mobility in the manufacturing process [1]. Monitoring the stress in the local area over the whole surface of wafer will accelerate the development speed of devices and contribute the yield enhancement in the process.

This paper presents a new impact of micro-Raman spectroscopic metrology tool for stress measurement, which is available for 300mm wafer in the manufacturing process. By using this metrology tool, we evaluated an influence of $SiO_2$ composition embedded in μm scale shallow trench isolation (STI) on the local stress variation. And, the stress variation caused by the difference of the trench depth and the crystal orientation of silicon in the nm scale pattern were researched by this tool.

## 2. Raman Spectroscopy and Metrology tool

Raman spectrum for single crystal silicon appears at 520.5cm$^{-1}$. It should be noted that the peak position of Raman spectrum has a linear relation to stress or strain of silicon. In the case of biaxial stress in silicon, the relation between the peak shift and the stress is expressed as;

$$\sigma_{xx} + \sigma_{yy} = a \times \Delta\nu \qquad \text{(MPa)} \qquad (1)$$

Here, Δ is the peak shift difference between non -stressed silicon and stressed one. And, $a$ is the shift-stress coefficient for silicon, which is 232MPa/cm$^{-1}$ [2].

All Raman measurements were done with HORIBA Automatic Raman Spectroscopic Metrology System (Model:FR-3000) which is mainly consists of LabRAM HR-800 of HORIBA Jobin Yvon and C to C wafer handling equipment. This micro-Raman spectrometer has a real confocal optics and a spectrograph with long focal length (800mm). The pattern recognition function with the positioning accuracy of sub-μm is available. The excitation line is 363.8nm of Ar ion laser, which the minimum laser spot size is ~0.5μm and the penetration depth is ~10nm in silicon.

## 3. Stress Measurement in Memory Devices

Figure 1 shows schematic diagrams of a cross section and SEM photograph of μm scale STI fabricated on the 300mm wafer. Two wafers that the stress state is different depending on the composition of $SiO_2$ were manufactured. 2-Dimensional stress distributions for the micro pattern including STI structure are shown in figure 2. A positive and a negative value in this figure refer to compressive and tensile stress, respectively. We can see that there is the stress distribution corresponding to μm pattern in both wafers, i.e., the difference of stress state in sub-μm pattern can be detected by this metrology tool. And, the compressive and tensile stresses are confirmed on A-1 and A-2 wafer, respectively. This difference of stress state agrees with the manufacturing intention.

Line step measurements for μm square pattern indicated in figure 1 were performed for verifying a distribution on the wafer. A typical stress distribution of these measurements for A-2 wafer is shown in figure 3(a), and fig.3 (b) shows the mean stress value at the top, the center, and the bottom. The compressive stress of 200MPa and the tensile stress of -200MPa are confirmed on A-1 and A-2 wafer, respectively. And, it is found that the stress at the center is slightly higher than that at the top and the bottom.

We also conducted the measurement for nm scale cell pattern on 4 wafers in order to confirm the influence of the depth of STI and the crystal orientation of silicon on the stress. Table 1 and figure 4 show the pattern specification and the SEM photograph of the cell area that has periodical rectangle patterns in nm scale. The laser spot size for these measurements was 10x10μm by using scanning laser technique and the acquisition time for one area was 6 seconds. In this case, obtained stress was mean value for the top surface of several patterns. Figure 5 shows the stress value of each area. Regarding the stress over wafer surface for B-1, 2, 3, the tensile stress ranging in -50~0MPa is induced at the top and the bottom, and the stress at the center is almost 0MPa. The inhomogenity of $SiO_2$ deposition over the wafer may cause these stress deviations.

Considering the influence of the trench depth, there is a clear difference between B-1 and B-2 wafer. The stress on B-2 wafer indicates 20MPa tensile side compared to B-1 in all measurement region. The tensile stress in deep STI seems to be higher than that in the shallow STI. And, the stress state strongly depends on the crystal orientation of the cell area. Only B-4 which varies the crystal orientation indicates high compressive stress, which is about 250MPa.

## 4. Conclusion

This paper reveals the effectiveness of Raman Spectroscopic Metrology tool for measuring the local stress on

300mm patterned silicon wafer. From these measurement results for μm/nm scale STI pattern, it is found that this tool is clearly able to verify the difference of the stress status of silicon caused by the difference of $SiO_2$ composition, the trench depth, and the crystal orientation.

Moreover, Raman spectroscopy had been proven to be suitable evaluation technique for not only single crystal silicon but also other materials, such as poly-Si, compound semiconductor(Silicon Germanium[3]),Carbon(CNT, DLC), and so on. That is, this new industrial solution for the stress has a great possibility to adapt to various applications, es

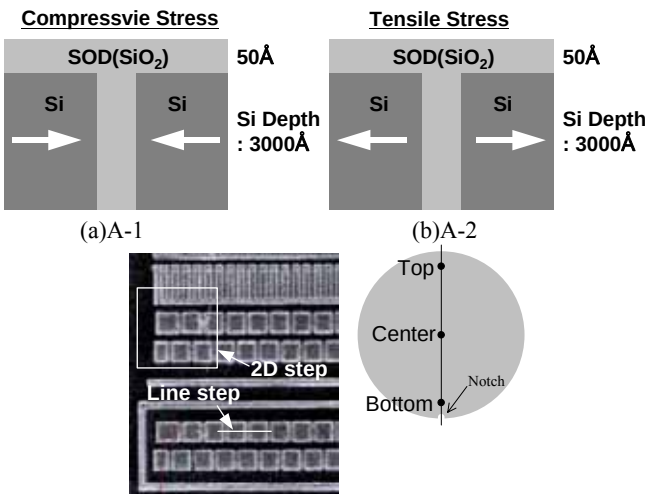


(a)A-1 (b)A-2

(c)Measurement area

Figure 1 Schematic of cross section of STI structure / predicted stress state on A type wafer and measurement area

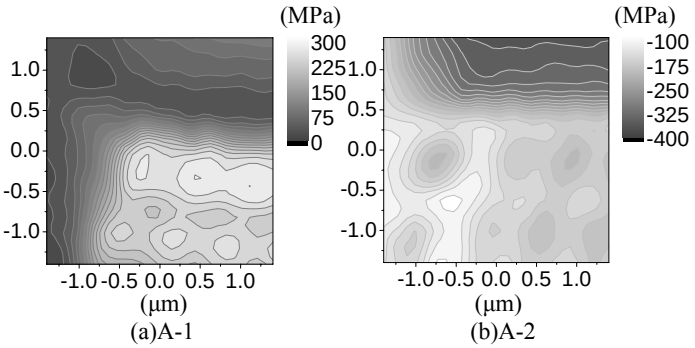


(a)A-1 (b)A-2

Figure 2 2-dimensional stress distributions around STI for A sample wafers.

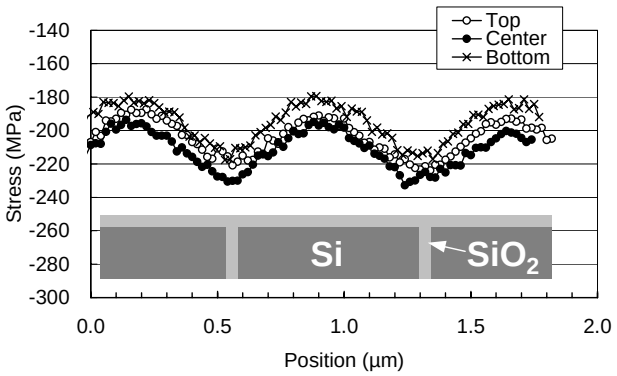


Figure 3 (a) Typical stress distribution along the line on STI structure for A-2 wafer.

pecially the crystallinity evaluation, in the future manufacturing process as well.

## References


[1] ITRS Roadmap, Metrology, 21 (2007).

[2] N.Naka,S.Kashiwagi,Y.Nagai,T.Namazu, S.Shimada, K.Ohtsuki, Ext.Abstra. 2007 Int'l Conf. on Solid State Devices and Materials, 392, (2007).

[3] J.C.Tsang, P.M.Mooney, F.Dacol, J.O.Chu, "Measurements of alloy composition and strain in thin GexSi1-x layers", J.Appl.Phys., 75, 8098 (1994).


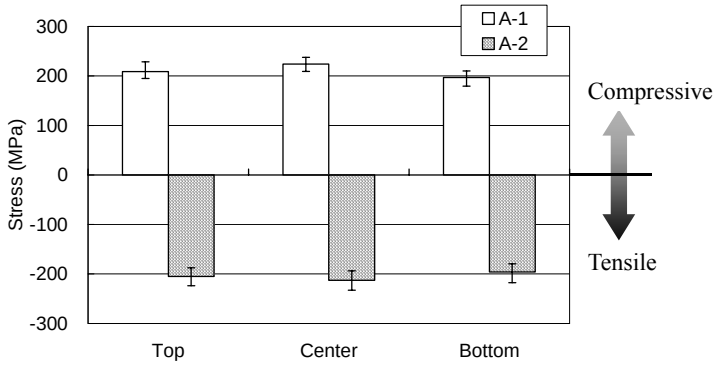


(b) Mean stress of STI structure

Figure 3 Stress evaluation result of STI structure for A sample wafers.

Table 1 Specification of cell pattern.

| Wafer | Trench depth (Å) | Cell isolation angle (deg) | Notch angle (deg) |
|---|---|---|---|
| B-1 | 4000 | 0 | 0 |
| B-2 | 4600 | 0 | 0 |
| B-3 | 4000 | θ | 0 |
| B-4 | 4600 | θ | θ |


Cell isolation angle : 0 Cell isolation angle : θ

Figure 4 Cell structure of B type wafer.
(Right picture for only B-4 wafer)

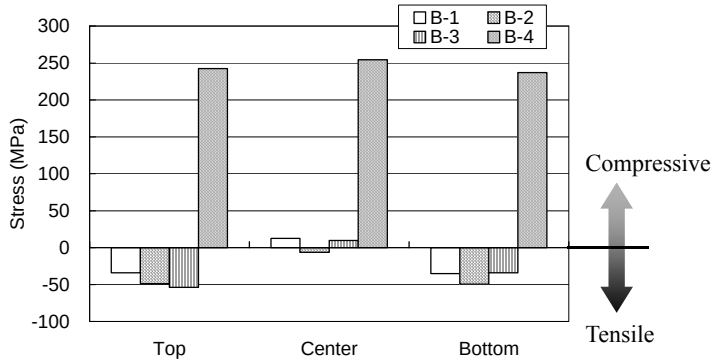


Figure 5 Stress evaluation result of cell structure for B sample wafers.